

MAppleT: simulation of apple tree development using mixed stochastic and biomechanical models

Evelyne Costes^{A,F}, Colin Smith^A, Michael Renton^D, Yann Guédon^{B,C},
Przemyslaw Prusinkiewicz^E and Christophe Godin^{B,C}

^AINRA, UMR 1098 CIRAD-INRA-Montpellier SupAgro-UM2, 2 Place Viala, F-34060 Montpellier, France.

^BCIRAD, UMR 1098 CIRAD-INRA- Montpellier SupAgro-UM2, Avenue Agropolis, TA A96/02, F-34398 Montpellier, France.

^CINRIA, Equipe Virtual Plants, Avenue Agropolis, TA A96/02, F-34398 Montpellier, France.

^DSchool of Plant Biology, Faculty of Natural and Agricultural Sciences, The University of Western Australia, Crawley, WA 6009, Australia.

^EDepartment of Computer Science, University of Calgary, Alberta, T2N 1N4, Canada.

^FCorresponding author. Email: costes@supagro.inra.fr

This paper originates from a presentation at the 5th International Workshop on Functional–Structural Plant Models, Napier, New Zealand, November 2007.

Abstract. Construction of tree architectural databases over years is time consuming and cannot easily capture event dynamics, especially when both tree topology and geometry are considered. The present project aimed to bring together models of topology and geometry in a single simulation such that the architecture of an apple tree may emerge from process interactions. This integration was performed using L-systems. A mixed approach was developed based on stochastic models to simulate plant topology and mechanistic model for the geometry. The succession of growth units (GUs) along axes and their branching structure were jointly modelled by a hierarchical hidden Markov model. A biomechanical model, derived from previous studies, was used to calculate stem form at the metamer scale, taking into account the intra-year dynamics of primary, secondary and fruit growth. Outputs consist of 3-D mock-ups – geometric models representing the progression of tree form over time. To assess these models, a sensitivity analysis was performed and descriptors were compared between simulated and digitised trees, including the total number of GUs in the entire tree, descriptors of shoot geometry (basal diameter, length), and descriptors of axis geometry (inclination, curvature). In conclusion, despite some limitations, MAppleT constitutes a useful tool for simulating development of apple trees in interaction with gravity.

Additional keywords: biomechanics, functional–structural plant model, *Malus × domestica*, Markov model, tree simulation.

Introduction

In the last 20 years, the introduction of architectural studies in horticulture has led to a better understanding of fruit tree development and to improvements of tree management at the orchard level (Lauri 2002; Costes *et al.* 2006). In particular, tree architecture plays a key role in 3-D foliage distribution and consequently in light interception and carbon acquisition, which in turn strongly affect the reproductive growth of fruit trees. During tree ontogeny, tree architecture is progressively built up, reflecting a complex interplay between the topology of tree entities (which, in turn, results from the growth and branching processes) and their geometry, including both the shapes and 3-D positions of these entities (Godin 2000). Specific methodologies have been proposed to capture tree topology (Hanan and Room 1997; Godin and Caraglio 1998) and geometry (Sinoquet *et al.* 1997), and to combine both descriptions (Godin *et al.* 1999). Based on these methodologies, several databases have been built for several cultivars of apple tree, and models have been

developed for analysing growth and branching processes along the trunks (Costes and Guédon 2002), the branches (Lauri *et al.* 1997), and over tree ontogeny (Costes *et al.* 2003; Durand *et al.* 2005; Renton *et al.* 2006). In parallel, the question of stem form change over time has been addressed by the development of biomechanical models (Fournier *et al.* 1991a, 1991b; Jirasek *et al.* 1991b, 2000; Ancelin *et al.* 2004; Taylor-Hell 2005). Fournier *et al.* (1991a, 1991b) clarified the application of mechanical principles to the calculation of the deformation of a growing stem. These works underlined the importance of the relative dynamics of stem loading and rigidification. An extension of this model to the bending of fruit tree branches has been applied to the apricot tree and required to take into account the intra-year dynamics of growth, loading and rigidification (Almérés *et al.* 2002).

As the construction of architectural databases over years is time consuming and cannot easily capture the dynamics of events, especially when both topology and geometry are considered, we

developed a complementary strategy which aims to integrate the acquired knowledge into simulations of a developing tree architecture. Our project was to bring together the models of topology and geometry development into a single simulation, such that the architecture of an apple tree may emerge from these models interacting over time. This integration was accomplished using an L-system simulation model, MAppleT, which is presented in this paper.

In previous studies, L-systems (Lindenmayer 1968; Prusinkiewicz and Lindenmayer 1990) have been widely used to simulate various aspects of plant development (Prusinkiewicz 1998). In many applications, local rewriting rules apply to apical meristems to model meristem production at the metamer scale (as defined by White 1979). In these simulations, mechanistic models of plant function specified at various levels of abstraction have been applied to simulate diverse plants. For instance, the allocation and transport of carbon has been considered in peach (Allen *et al.* 2005; Lopez *et al.* 2008); the relationship between plant structure, fruiting patterns and environment, and the effect of defoliation on plant structure have been addressed in cotton (Hanan and Hearn 2002; Thornby *et al.* 2003); and the impact of light has been considered in various coniferous and deciduous trees (Mech and Prusinkiewicz 1996; Renton *et al.* 2005a, 2005b) and in clover (Gautier *et al.* 2000). In the present study, we developed a mixed approach based on stochastic models for representing plant topology, and mechanistic model for the geometry. The modelling of branch bending critically depends on the distribution of masses along the branch (e.g. fruits, and long or short shoots). As current mechanistic models do not represent axillary distribution with sufficient precision, we used stochastic models (Guédon *et al.* 2001; Guédon 2003) to simulate axillary and terminal bud fate at the growth unit scale (GU). A growth unit is defined as a succession of metamers built during a growing period, i.e. between two resting period of the meristem; a GU is limited by scars indicating the growth slowing down or stopping (Hallé and Martin, 1968). This scale makes it possible to account for tree development in consecutive years, and for phenomena which have a particular importance to fruit trees, such as the annual regularity (or alternation) of fruit production and the distribution of fruit within the tree structure. Regarding stem form, calculations were performed at the metamer scale, taking into account the intra-year dynamics of primary, secondary and fruit growth. The bio-mechanical model used in MAppleT is derived from the work by Jirasek *et al.* (2000) and Taylor-Hell (2005), and from the work by Alméras (2001) and Alméras *et al.* (2002, 2004). These works are based in turn on the metaphor by Fournier (1991a, 1991b) of bending beams applied to woody stems.

In MAppleT, tree architecture is determined by two types of information: the tree topology (i.e. the connections between plant entities, such as the sequence of GUs and the placement of the organs) and the temporal coordination of developmental events, the latter including both morphogenesis and organ growth. From this information, the tree geometry is determined by computing the biomechanics of the tree. Our goal was to lay out the foundations for a fruit tree simulation program that would make it possible to examine virtual scenarios of horticultural practices, considering genetic variation of architectural traits. Given the high complexity of possible model outputs, our aim

was to initiate a validation approach by defining several tree descriptors and comparing them between simulated and digitised trees. This paper presents (i) the datasets that were used in the modelling approach, (ii) the elementary models that were integrated in MAppleT simulations, and (iii) the results of simulations, which were obtained in both graphical and numerical form.

MAppleT: an integrated simulation model

Plant material

Our main database consisted of data for two apple trees (*Malus × domestica* Borkh), cultivar Fuji, the topology and geometry of which were entirely described over 6 years (Costes *et al.* 2003; Durand *et al.* 2005). The method used to describe tree topology was detailed by Godin *et al.* (1999) and Costes *et al.* (2003). In brief, each tree was described using three scales of organisation corresponding to axes, GUs, and metamers. Two types of links between plant components were considered: succession and branching. Three axis types (long, medium and short) were distinguished, depending on their composition in term of GUs. These GUs were divided into four categories. (1) Long GUs were more than 20 cm long and had 22 metamers on average. They included both preformed and neoformed elongated internodes. (2) Medium GUs were more than 5 cm but less than 20 cm long. These GUs consisted of eight metamers on average, which were typically preformed and had elongated internodes. (3) Short GUs were less than 5 cm long, and consisted of non-elongated, preformed organs. (4) Floral GUs or 'bourses' resulted from floral differentiation of the apical meristem. The number of metamers was counted on the long and medium GUs only.

In this database, the tree geometry was obtained by digitising the woody axes in autumn. The trees were described three times, in their fourth, fifth and sixth year of growth. Spatial coordinates and diameters were measured at the metamer scale, each five nodes along the long and medium GUs, and at the top of short axes. Spatial coordinates were collected using 3-D FastTrack (Polhemus Inc., Cochester, VT, USA) digitiser and 3A software (Adam *et al.* 1999). Using this database, which combined both topological and geometrical observations, 3-D reconstructions of the trees were obtained with V-Plants software (formerly AMAPmod; <http://www-sop.inria.fr/virtualplants/wiki/doku.php?id=software>, accessed 2 September 2008), in order to compare them with simulated outputs of geometrical models.

Additional data from other experimental designs, collected mainly on the Fuji cultivar, were used in complement, especially for the plastochron value, dynamics of diameter growth, and the wood properties of axes. References to these data are indicated in the text.

Model for tree topology

In MAppleT, the topology of the trees was simulated using stochastic models. The succession of GUs along axes and the branching structure of GUs were jointly modelled by a two-scale stochastic process that was inspired by the hierarchical hidden Markov model proposed by Fine *et al.* (1998). At the macroscopic GU scale, the succession of GUs along axes is modelled by a four-

state Markov chain. The four ‘macro-states’ are long, medium, short and flowering GU (Fig. 1). This Markov chain is indexed by the GU rank along axes and is defined by two subsets of parameters:

- (1) initial probabilities, needed to model which is the first GU occurring in the axis (the set of initial probabilities constitutes the initial distribution):

$$\pi_y = P(GU_1 = y) \text{ with } \sum_y \pi_y = 1,$$

- (2) transition probabilities, to model the succession of GUs along axes (the set of probabilities corresponding to the transitions leaving a given macro-state constitutes the transition distribution of this macro-state):

$$p_{xy} = P(GU_n = y | GU_{n-1} = x) \text{ with } \sum_y p_{xy} = 1.$$

At the microscopic metamer scale, branching structures of long and medium GUs are modelled by hidden semi-Markov chains (HSMCs) that are indexed by the node rank along GUs. A HSMC is defined by four subsets of parameters:

- (1) initial probabilities, needed to model which branching zone is the first one in a GU (of type y):

$$a_{yj} = P(S_1 = j | GU_n = y) \text{ with } \sum_j a_{yj} = 1,$$

- (2) transition probabilities, to model the succession of branching zones along a GU:

$$q_{ij} = P(S_t = j | S_t \neq i, S_{t-1} = i) \text{ with } \sum_{j \neq i} q_{ij} = 1,$$

- (3) occupancy distributions, to model the lengths of branching zones in number of metamers:

$$d_j(u) = P(S_{t+u+1} \neq j, S_{t+u-v} = j, v = 0, \dots, u-2 | S_{t+1} = j, S_t \neq j) \quad u = 1, 2, \dots,$$

- (4) observation distributions, to model the branching type composition of branching zones:

$$b_{jy} = P(GU_1 = y | S_t = j) \text{ with } \sum_y b_{jy} = 1.$$

During the simulation, transitions between scales (a_{yj} and b_{jy}) and within scales (p_{xy} and q_{ij}) are managed through a precise

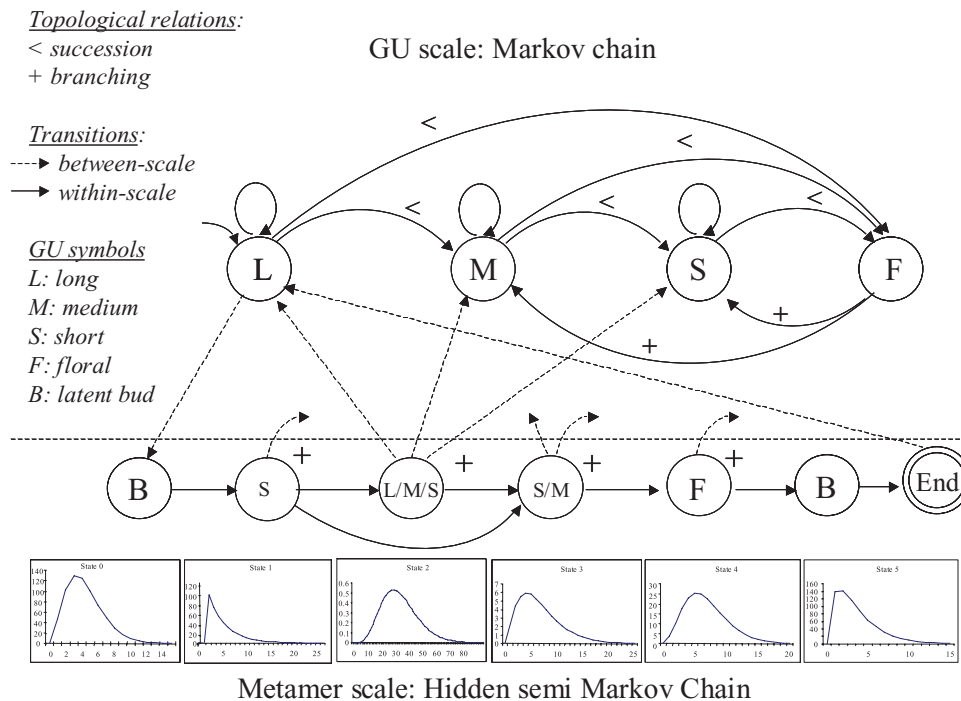


Fig. 1. Hierarchical stochastic model representing tree topology. Successions and branching between entities are represented by ‘<’ and ‘+’, respectively. At the growth unit (GU) scale, the succession of GUs along an axis is modelled by a 4-state Markov chain. The four ‘macro-states’ are long (L), medium (M), short (S) and flowering (F) GU. The long and medium macro-states activate HSMCs with between-scale transitions (dotted arrows). The figure shows only the activation from the long GU macro-state. HSMCs model the GU branching structure at the metamer scale, as a succession of zones with a specific composition of axillary GUs (for instance a mixture of long, medium and short axillary GUs is observed in state 2). The HSMC ends with an artificial final state which gives control back to the pending macro-state. Likewise, for each axillary position, between-scale transitions give the control back to the macro-state model corresponding to the type of axillary GU generated by the HSMC (the figure illustrates only these transitions from HSMC state 2).

scheduling scheme that distinguishes this hierarchical model from the standard hidden Markov models. When entering a long or medium GU macro-state, the associated HSMC is activated first (Fig. 1). The initial state is selected according to the initial distribution of the HSMC, and this corresponds to a between-scale transition $a_{y,j}$. The succession of branching zones along the GU is then modelled at the metamer scale using the within-scale transitions of the HSMC. The HSMC simulation determines the type of axillary GU at the metamer scale. This process ends with an artificial final state from which the control returns to the macro-state that has activated the HSMC. This corresponds to another between-scale transition. The type of next GU is then chosen according to the within-scale transition distribution of the current macro-state. For a given GU, its successor and axillary GUs are simulated in parallel, thus generating a growing tree structure. These GUs develop according to a calendar that defines the dates at which the different processes occur (see below). The beginning of the simulation of a new axillary GU in a given macro-state also corresponds to a between-scale transition $b_{j,y}$. We note that, in this approach, the GU length, measured in the number of metamers, is not simulated on the basis of a known *a priori* distribution, but results from adding up the lengths of the branching zones (simulated according to the corresponding state occupancy distributions of the HSMC).

In MAppleT, we assume that the simulation begins in the first year of growth with a trunk in the long GU macro-state. In the following years, if the first GU of the year is vegetative, we assume that it does not give rise to another GU in the same year. This means that polycyclism, i.e. the capability to develop several vegetative GU in the same growing season was not taken into account in our study, consistent with the reduced polycyclism in Fuji (Costes *et al.* 1995). In contrast, if the first GU developed in a given year is floral, it may give rise in the same year to a vegetative GU, which, in this case, develops immediately (Crabbé and Escobedo-Alvarez 1991).

Estimation of Markov chain parameters

From the database described above, sequences of GUs were extracted along all axes, including the trunks, to estimate the parameters of the macro-state model. After flowering, the new axis arising from sympodial branching was considered as the continuation of the previous axis. When two axes arose from the same floral GU, the distal one was chosen as the continuation. Sequences of GUs were then modelled by a first-order Markov chain. Since it has been demonstrated that transitions between GUs change with tree ageing due to tree ontogeny (Durand *et al.* 2005), the transition probability matrices between GU types were estimated annually from the second to the sixth year of growth (Table 1). When long GUs were considered, few or no transitions towards short GU or meristem death took place in any year, and the most frequent transitions were towards another long or a floral GU. When medium GUs were considered, the most frequent successor in all years was a floral GU. A small number of medium GUs was followed by another medium GU, and an even smaller number was followed by a long GU. Direct transitions towards a short GU or death were rare. When the parent GU was short, the most frequent transitions were towards another short or a floral

GU, depending on the year. This change in transitions with years resulted from the alternating flowering behaviour of Fuji cultivar (Costes *et al.* 2003). The transitions from floral GU towards long GU decreased from the second to the fourth year of growth, and those towards medium GU increased. However, the most frequent transitions from floral GU were towards short GU or meristem death.

Similarly, axillary bud fates were explored during tree ontogeny, for different GU types and years of growth, in order to estimate the parameters of HSMC (Renton *et al.* 2006). In previous studies, the branching pattern along 1-year-old trunks was shown to be organised into successive zones, and hidden semi-Markov chains were proposed to model this structure (Costes and Guédon 2002). This approach was further extended to explore how branching patterns, described at the metamer scale along GUs, change during tree ontogeny. From the initial database, all GUs of the two Fuji trees were extracted and classified by type, year of growth and branching order. For each GU, the axillary bud fates were observed metamer by metamer and represented as a sequence of symbols corresponding to five types of lateral growth (latent bud, and short, medium, long, or floral lateral GUs). First, all these sequences were used to estimate a single HSMC composed of six successive transient states followed by an 'end' state [Fig. 1; see Renton *et al.* (2006) for details on model building]. Second, each observed sequence was optimally segmented into branching zones, using the estimated HSMC. Bivariate sequences were built by associating each observed sequence with the corresponding optimal segmentation into branching zones. The resulting bivariate sequences were grouped hierarchically according to the GU length, year of growth, and branching order. Parameters were estimated for each group of bivariate sequences on the basis of counts for the transition between successive branching zones, the branching zone length and the branching type composition of branching zones. The comparison of model parameters between these groups highlighted similarities between GUs: the composition and relative position of the latent bud, floral and short-lateral zones were invariant within the GUs. The probability of occurrence of the floral zone changed over years, showing the alternative fruiting behaviour of the Fuji cultivar. Moreover, during ontogeny, branching patterns tended to become simplified due to the disappearance of the central zones and a progressive reduction of the floral zone length (Renton *et al.* 2006). To formalise these results in MAppleT, a single subset of parameters was used to represent mixtures of possible axillary GUs in the branching zones and occupancy distributions for zones that were the same for all GU types and years. In contrast, for zones that differed between GU types or years, different subsets of parameters were used for transition probabilities between zones and occupancy distributions depending on the GU type and year.

In HSMC, the length of the sequences is a property of the model and does not depend on the branch location. This may lead to unrealistic sequence length, ignoring the experimentally found decrease in the number of metamers per GU with tree age (Costes *et al.* 2003). Consequently, we extracted the empirical distribution of number of metamers per GU from the initial database (Fig. 2). On the basis of this distribution, we selected limits for the range of sequence lengths according to the GU type and year of growth. The sequences generated by HSMC were then

Table 1. Transition probabilities between successive growth units (GUs), with associated counts and 95% confidence intervals into brackets, depending on the year of growth for two apple trees, cultivar Fuji

Four types of GU were considered: long GU (L), medium GU (M), short GU (S) and floral GU (F). Successor GU after a floral GU arose from sympodial branching. x indicates an impossible transition

Years, parent– successor	Count	Parent	Successor				Death
			L	M	S	F	
2–3	12	L	0.5 (0.22, 0.78)	0.17 (0, 0.38)	0	0.33 (0.07, 0.6)	0
	1	M	0	0	0	1	0
	9	S	0.45 (0.12, 0.77)	0	0	0.44 (0.12, 0.77)	0.11 (0, 0.32)
	6	F	0.33 (0, 0.71)	0	0.5 (0.1, 0.9)	x	0.17 (0, 0.46)
Total	28						
3–4	65	L	0.25 (0.14, 0.35)	0.18 (0.09, 0.28)	0	0.57 (0.45, 0.69)	0
	64	M	0.02 (0, 0.05)	0.23 (0.13, 0.34)	0.03 (0, 0.07)	0.7 (0.59, 0.82)	0.02 (0, 0.05)
	60	S	0.07 (0, 0.13)	0.07 (0, 0.13)	0.31 (0.2, 0.43)	0.55 (0.42, 0.68)	0
	96	F	0.20 (0.12, 0.28)	0.16 (0.08, 0.23)	0.27 (0.18, 0.36)	x	0.37 (0.28, 0.47)
Total	285						
4–5	98	L	0.34 (0.24, 0.43)	0.1 (0.04, 0.16)	0.01 (0, 0.03)	0.51 (0.41, 0.61)	0.04 (0, 0.08)
	139	M	0.11 (0.06, 0.17)	0.14 (0.08, 0.19)	0.06 (0.02, 0.1)	0.62 (0.54, 0.7)	0.07 (0.03, 0.11)
	526	S	0.01 (0, 0.02)	0.08 (0.06, 0.11)	0.4 (0.36, 0.44)	0.39 (0.34, 0.43)	0.12 (0.1, 0.15)
	532	F	0.11 (0.08, 0.13)	0.15 (0.12, 0.18)	0.33 (0.3, 0.38)	x	0.41 (0.37, 0.45)
Total	1295						
5–6	61	L	0.21 (0.11, 0.32)	0.08 (0.01, 0.15)	0	0.71 (0.59, 0.82)	0
	324	M	0.02 (0.01, 0.04)	0.04 (0.02, 0.07)	0.02 (0, 0.03)	0.85 (0.81, 0.89)	0.07 (0.04, 0.1)
	1234	S	0	0.02 (0.01, 0.03)	0.15 (0.13, 0.17)	0.58 (0.55, 0.61)	0.25 (0.22, 0.27)
	615	F	0	0.27 (0.24, 0.31)	0.39 (0.35, 0.42)	x	0.34 (0.3, 0.38)
Total	2234						

accepted or rejected depending on the correspondence between their length and the range of possible lengths for each GU type and year of growth.

Chronological control of morphogenesis and organ dimensions

In MAppleT, a calendar defines the starting dates of simulated processes, i.e. primary and secondary growth (Fig. 3). However, individual organs at the metamer scale develop according to their own chronology, as they appear during the whole season. In each GU category, new metamers are produced with a plastochron of 3 days. This value corresponds to the mean observed over a growing season for two different apple tree cultivars, ‘Starkrimson’ and ‘Rome Beauty’, grown with two different rootstocks (Costes and Lauri 1995). The period over which a

metamer elongates was set to 10 days according to observations by J. J. Kelner (pers. comm.). Measurements conducted on Fuji cultivar (M. Renton, E. Costes, Y. Guédon, unpubl. data), showed that the final length of internodes depended on the internode position in the shoot, such that the internodes at the beginning and end of each GU were shorter than those in the middle. In MAppleT, this variation was modelled by attributing different lengths to internodes according to the branching zone along the shoot to which they belong.

Following field observations of Fuji leaf development collected by Massonnet (2004), it was assumed in MAppleT that leaves grow sigmoidally over 12 days, at which time they reach maturity. Similarly, according to field observations of flowering and harvest dates in Fuji (J.L. Regnard, pers. comm.), we assumed that, if a metamer supports an inflorescence, the flowers last for 10 days, and if it becomes a

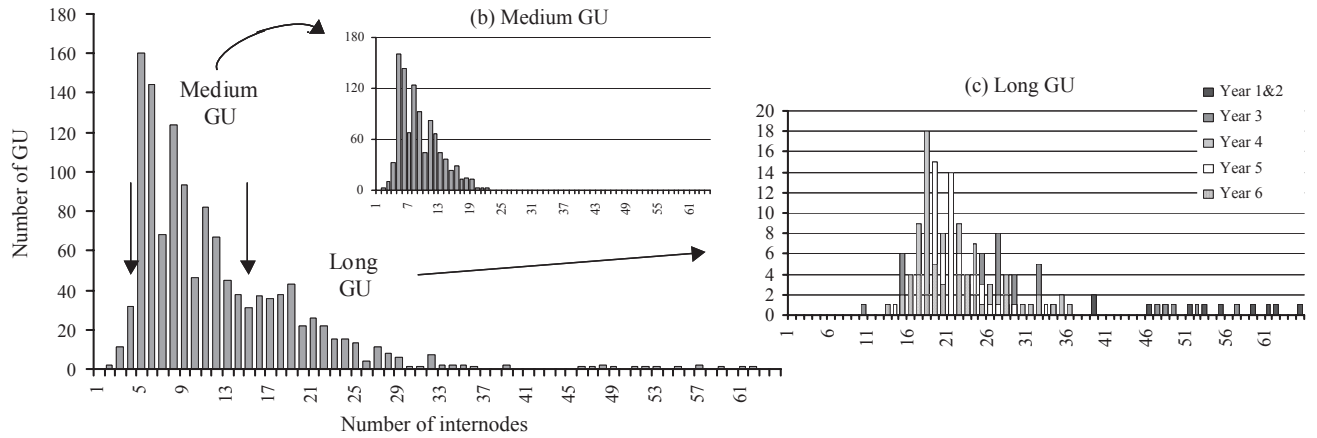


Fig. 2. Relationship between GU type and limits used in MAppleT to partition the sequence lengths (i.e., the number of internodes per GU) into classes. Based on the distributions of the number of internodes for medium and long GU (Fig. 1b, c), the boundary between medium and long GU was fixed at 15 internodes (indicated by the arrow at the 15th node). According to the distributions of the number of internodes per year for long GU (Fig. 1c), the maximum possible length decreased with the year of growth.

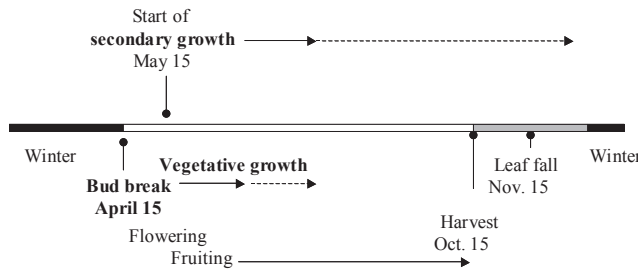


Fig. 3. Calendar of simulated events over a year in MAppleT. In this calendar, new metamers develop with a plastochrone of 3 days, and each organ (i.e. leaves, internodes, flowers, and fruits) has its own chronology for development.

fruit, the fruit lasts until harvest (~150 days). We also assumed that each inflorescence develops into one fruit at most, which corresponds to the usual thinning practices (Costes *et al.* 2006). An expolinear model, i.e. an exponential function followed by a linear function, had been proposed by Lakso *et al.* (1995) to estimate the increase in mass of a fruit over time, and was calibrated to the fruit of Fuji during a previous study (Massonnet 2004). This expolinear model with parameters for Fuji was used in MAppleT.

As large and rapid bending of axes is usually observed in fruit trees over a fruiting season, the intra-year dynamics of diameter growth must be taken into account in biomechanical computations (Alméras *et al.* 2004). In MAppleT, the widths of the internodes were controlled in the spirit of the pipe model proposed by Shinozaki *et al.* (1964). In particular, we used the metaphor introduced by these authors that considers each distal end of a plant as an origin of a vascular strand (a ‘pipe’), and that at each branching point, these strands are bundled together to form a larger, composite strand. According to this metaphor and a formulation proposed by Murray (1927) and further analysed by MacDonald (1983), the radius, r of an internode is determined by the formula $r^P = r_a^P + r_b^P$, where r_a corresponds to a lateral internode borne on the current internode, r_b to the internode

following the current internode along the axis, and P is a fixed parameter, which we call the pipe model exponent. However, Suzuki and Hiura (2000) showed that this model explains allometry relationship at the level of the whole tree, but does not always apply to the current shoot. In particular, the pipe model formulation implies that growth in diameter occurs only when new internodes are added. To verify this assumption, we used a previously collected dataset of 1-year-old floral GUs of Golden Delicious cultivar (Benzing 1999). This dataset characterised both the within-year dynamics of primary growth, i.e. number of new metamers, and growth in diameter (Fig. 4). Observations showed that primary growth of the shoots was found to start in mid-April and stop at the beginning of June. The diameter at the shoot base increased over the growing season in two distinct periods: rapidly from bud burst to the end of May and more slowly from mid-June to the end of the growing season. This demonstrated that growth in diameter continues even after the cessation of primary growth. Moreover, in a previous study conducted on an apricot tree, the basal diameter of 1-year-old shoots was found to be linearly related to the number of internodes, independently of the fruit load (Costes *et al.* 2000). Following these experimental data, we modelled the secondary growth in MAppleT by augmenting the diameter of the terminal internode continuously after the cessation of primary growth. This was done using the formula,

$$r_a(s) = r_{a,\min} + (r_{a,\max} - r_{a,\min}) \left(\frac{n(s) - n_{\min}}{n_{\max} - n_{\min}} \right), \quad (7)$$

where $r_a(s)$ is the radius of the terminal internode of shoot s at the end the growing season, $r_{a,\min}$ is the initial radius of this internode upon its creation (set to 0.75 mm, Table 2), $r_{a,\max}$ is the maximum radius observed at the end of the growing season for any terminal internode ($r_{a,\max}$ was set to 6 mm according to field observations), $n(s)$ is the number of internodes of shoot s at the end of primary growth, and n_{\min} and n_{\max} are the minimum and maximum numbers of metamers observed in the population

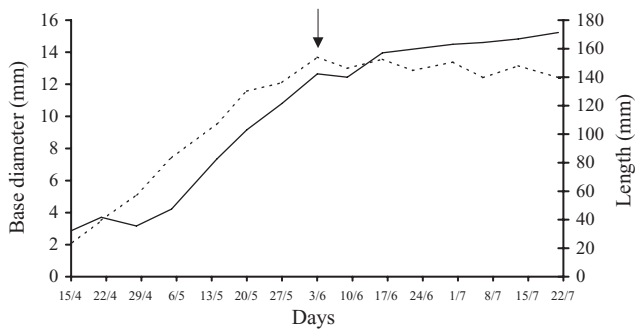


Fig. 4. Increase in the mean base diameter (left axis and continuous line) and length (right axis and dotted line) of 1-year-old GU over a growing season, in the apple tree cultivar ‘Golden Delicious’ (data from Benzing 1999). The arrow indicates the primary growth cessation.

of shoots of the same type as s . Thus, $r_a(s)$ is located between $r_{a,\min}$ and $r_{a,\max}$ proportionally to the status of shoot s in the population, as defined by its number of metamers.

Determination of plant geometry using biomechanics

In MAppleT, the shape of each branch is calculated according to the biomechanical component of the model. Our method simulates branch bending and twisting, and the resulting

permanent changes of branch shape (‘shape memory’), following Fournier’s treatment of woody stems as elastic beams (rods) subject to primary and secondary growth (Fournier 1989; Fournier *et al.* 1991a, 1991b). L-system implementations of Fournier’s model were originally developed by Jirasek *et al.* (2000) and Taylor-Hell (2005); a tutorial introduction to biomechanical modelling using L-systems is also presented by Prusinkiewicz *et al.* (2007). Mathematically, the equations used in our approach represent a finite-difference discretisation of the underlying partial differential equations (Jirasek *et al.* 2000), which capture the mechanics of elastic rods (Landau and Lifshitz 1986). We have chosen finite differencing over finite element methods because finite differencing is fully applicable to linear and branching structures, and is simpler to implement.

The use of L-systems does not introduce new elements to the mechanics of Fournier’s model, but facilitates the organisation of computation by seamlessly updating the system of equations that need to be solved when new metamers are added, and by integrating all aspects of MAppleT within a single software environment. The biomechanical component of MAppleT incorporates changes in shape due to the formation and impact of reaction wood, changes in the mechanical properties of wood with time, and the loading and unloading of fruits. The bending model is derived from the work by Taylor-Hell (2005), and

Table 2. List of parameters used in MAppleT

Parameters used in the sensitivity analysis are indicated by *. Default values are indicated for each parameter. The range of variation and the number of steps between minimum and maximum values tested in the sensitivity analysis are indicated only for the parameters used. This table does not include Markovian model parameters

	Name*	Symbol	Default value	Min–max	Nb steps
<i>Vegetative development</i>					
Shoot	Plastochrone		3 d	–	–
	Internode elongation		10 d	–	–
	Internode length		0.5–3.0 cm	–	–
	Spur death probability		0.3	–	–
Leaf*	Minimum final area		10 cm ²	–	–
	Maximum final area		30 cm ²	–	–
	Development duration		12 d	–	–
	Mass per area		220 g/m ²	–	–
<i>Floral development</i>					
Flower	Duration		10 d	–	–
Fruit	Maximum absolute growth rate*	C_m^*	1.8 g/day*	1.0–2.0*	5*
	Maximum relative growth rate		0.167 g/g.day	–	–
	Probability of fruit set*	Fr_p	0.3*	0.1–0.3*	2*
	Lost time		28 d	–	–
	Max age		147 d	–	–
<i>Diameter growth</i>					
	Pipe model exponent*	P^*	2.49*	2.0–3.0*	4*
	Radius of leaf petiole*	r_l^*	0.6*	0.5–1.5*	3*
	Min. radius of apical meristem	$R_{a,\min}$	0.75	–	–
	Max. radius of apical meristem	$R_{a,\max}$	6.0	–	–
<i>Geometry</i>					
	Branching angle		–45°	–	–
	Phyllotactic angle		–144°	–	–
	Tropism*	\vec{T}^*	(0, 0.1, 0) N*	0.1–1.0*	5*
	Young modulus*	E^*	1.1 GPa*	1.0–7.0*	6*
	Coefficient reaction wood*	α^*	0.1*	0.01–2.0*	5*
	Reaction wood rate		0.5	–	–

changes in shape due to reaction wood and loading/unloading are derived from the work of Alm eras (2001), and Alm eras *et al.* (2002, 2004).

In the biomechanical model, each point of a shoot axis is associated with a moving $\vec{H}\vec{L}\vec{U}$ frame, three orthogonal unit-length vectors that indicate the heading, upward and left directions (Prusinkiewicz and Lindenmayer 1990; Prusinkiewicz *et al.* 2001). Bending and twisting correspond to rotations of this frame. The rate of rotation is expressed as

$$\Omega = \left\langle \frac{d\theta_H}{dl}, \frac{d\theta_L}{dl}, \frac{d\theta_U}{dl} \right\rangle,$$

where the individual derivatives represent the rates of rotation around the \vec{H} , \vec{L} , \vec{U} vectors, and l is a position along the shoot axis. For computational purposes, we assumed that each shoot axis is discretised into a sequence of rigid internodes connected at flexible nodes (joints) (Fig. 5). The mass of each internode is assumed to be concentrated at its distal node.

The shape of the axis depends on the torques acting on its nodes. When calculating these torques, two factors are initially taken into account: the force of gravity and a combined effect of photo- and gravitropism, which is abstracted as an orthotropic force. The gravity component of the torque $\vec{\tau}_{i-1}^g$ that acts on the proximal node of an isolated internode i is equal to

$$\vec{\tau}_{i-1}^g = l_i \vec{H}_i \times m_i \vec{g},$$

where l_i is the length of this internode, \vec{H}_i is its heading vector, m_i is the mass of the distal node, and \vec{g} is the gravity acceleration. This equation is recursively extended to an entire axis using the formula

$$\vec{\tau}_{i-1}^g = l_i \vec{H}_i \times M_i \vec{g} + \vec{\tau}_i^g$$

where $M_i = \sum_{k=i}^N m_k$ is the cumulative mass of the nodes in the distal part of the shoot following internode i (Prusinkiewicz *et al.*

2007). A further extension to branching structures is accomplished by adding torques from all branches originating at the same node (Fig. 5c).

The combined effect of phototropism and negative gravitropism is simulated by turning shoots upward (Hangarter 1997). Although phototropism may act on both elongating and non-elongating shoots (Matsuzaki *et al.* 2007), we only consider the elongating (leafy) internodes. Specifically, we assume that leafy nodes are subject of a torque

$$\vec{\tau}_{i-1}^t = l_i \vec{H}_i \times \vec{T},$$

where \vec{T} is a vector indicating the upward tropic direction (see Table 2). The total torque acting on a node of a leafy shoot is, thus,

$$\vec{\tau}_i = \vec{\tau}_i^t + \vec{\tau}_i^g.$$

To calculate the resulting change in frame orientation, we decompose torque $\vec{\tau}_i$ into components τ_{iH} , τ_{iL} and τ_{iU} that act along the \vec{H} , \vec{L} , \vec{U} axes at node i , find the corresponding rotations

$$\Omega_{iH}^r = \frac{\tau_{iH}}{R_{iH}}, \Omega_{iL}^r = \frac{\tau_{iL}}{R_{iL}} \text{ and } \Omega_{iU}^r = \frac{\tau_{iU}}{R_{iU}}$$

around these axes, and compose them into the combined rotation Ω_i^r (Jirasek *et al.* 2000). Assuming that the rotations Ω_{iH}^r , Ω_{iL}^r and Ω_{iU}^r are small, their composition does not significantly depend on the order of rotations, and thus is well defined (Goldstein 1980).

In the above formulae, R_{iH} is the torsional rigidity of the axis at node i , and R_{iL} and R_{iU} are flexural rigidities in the direction of \vec{L} and \vec{U} axes, assumed to coincide with the principal axes of the cross-section of the axis at node i . This assumption is automatically satisfied if the branches have circular cross-section and the distribution of material properties in the branches is radially symmetric, which we assume in the model. Note that, in spite of this symmetry,

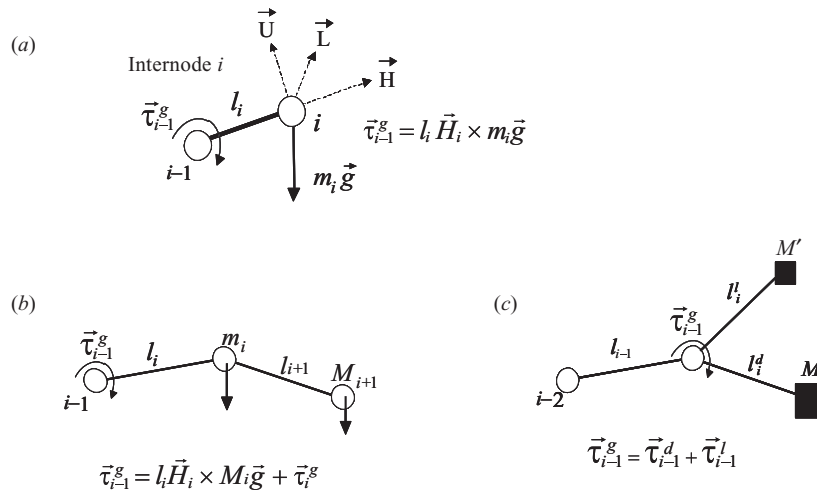


Fig. 5. Calculation of the torque due to gravity (g) acting on an internode. (a) Torque acting on the proximal end of an internode i with length l_i , loaded with a mass m_i at its distal end. (b) Recursive generalisation of the previous formula, where M_i is the cumulative mass of nodes located on the distal part of the shoot after internode i , and $\vec{\tau}_i^g$ is the torque acting on node i ; (c) generalisation of the torque calculation at a branching node.

branches may twist and bend out of vertical plane due to the presence of lateral branches. In principle, the flexural rigidity is calculated using the formula

$$R_{iL} = R_{iH} = EI$$

where E is the Young's modulus of the material, and I is the second moment of the area of the branch cross-section, equal to $(\pi/4)r^4$ for an axis passing through the centre of the circle of radius r (Niklas 1992). The torsional rigidity is calculated using an analogous formula,

$$R_{iH} = GJ,$$

where G is the shear modulus of the material, and J is a torsional constant, equal to $(\pi/2)r^4$ for a circle of radius r (Niklas 1992).

The bending of branches due to the combination of gravity and tropism, initially of elastic nature, leads to a permanent change of branch shape resulting from the memory effect of secondary growth, as discussed by Fournier *et al.* (1991a, 1991b) and Jirasek *et al.* (2000). The rotation Ω_i at node i is, thus, a linear combination of two terms: rotation Ω_i^r due to the current torque acting on this node, and rotation Ω_i^m due to the shape memory.

In MAppleT, we also assumed that some amount of reaction wood is produced each year in an angular section of the outer wood layer (Wilson and Archer 1977; Fig. 6a). The proportion of reaction wood in this layer is calculated using an empirical relation (Almérás 2001):

$$Pr = 0.164 - 0.178\Delta\theta,$$

where P_r is the proportion of reaction wood in the outermost cambial layer and $\Delta\theta$ is the change in shoot inclination in radians (i.e. the change in \vec{H} at each time step, which is negative when the branch bends). The way this formula is used in MAppleT relies on the assumption that the reaction wood does not play a major role in shape regulation in fruit trees, as previously demonstrated by Almérás *et al.* (2004) on different apricot cultivars. Here, the reaction wood is assumed to only prevent large bending

movements and, contrary to observations on several forest tree species, does not have any active up-righting function. Moreover, according to these previous observations on apricot tree, the amount of reaction wood also depends on the shoot orientation with respect to gravity, since an upright shoot develops less reaction wood than a leaning shoot (Almérás 2001). In MAppleT, a coefficient was thus introduced in order to make the amount of reaction vary with shoot orientation. The relationship used is:

$$P_r = 0.164(1 - \cos(\vec{H}, \vec{g}')) - 0.178\Delta\theta,$$

where \vec{g}' is a unit vector in the direction opposite to gravity. To keep the calculations simple, when reaction wood is present, it was assumed that the second moment of area of the initial cross-section is augmented with an additional contribution for each annular radial section of reaction wood (Fig. 6b). The contribution of the radial section of reaction wood to the section rigidity was assumed proportional to the moment of area calculated as follows:

$$I_s = \frac{1}{8}(r'^4 - r^4)(\gamma + \sin \gamma)$$

where γ is the angular section of reaction wood ($\gamma = 2\pi P_r$, in radians) in the cambial layer, and r and r' are the inner and outer radii respectively (Fig. 6b). The total second moment of area of an internode was thus expressed as

$$I = I_c + \alpha \sum_{k=1}^n I_{s,k}$$

where I_c is the moment of area for the whole cross-section, $I_{s,k}$ is the annular radial section of cambial layer k , and α is a coefficient that controls the reaction wood effect.

The biomechanical model was implemented in terms of information flow through the plant structure (Jirasek *et al.* 2000; Taylor-Hell 2005; Prusinkiewicz *et al.* 2007). The simulation is conducted by iterating two computational phases. First, bending and twisting moments are calculated in a backward scan of the L-system string (information is passed basipetally). In this phase, the torques $\vec{\tau}_i$ that apply to all internodes i are computed iteratively from the distal to the proximal end of the branch, given its current configuration. Second, the shape of the branch is updated in a forward (acropetal) scan of the string, taking bending moments and the resulting angles between the internodes into account. The consecutive node positions \vec{Q}_i are then calculated using the formula

$$\vec{Q}_{i+1} = \vec{Q}_i + l_i \vec{H}_i$$

This procedure is iterated until the position of the branch nodes converges towards a stable solution.

Simulation outputs

Owing to the stochastic nature of Markov models, different seeds used to initialise MAppleT's random number generator result in different topologies of simulated trees. These differences propagate to the level of tree geometries, which vary even if

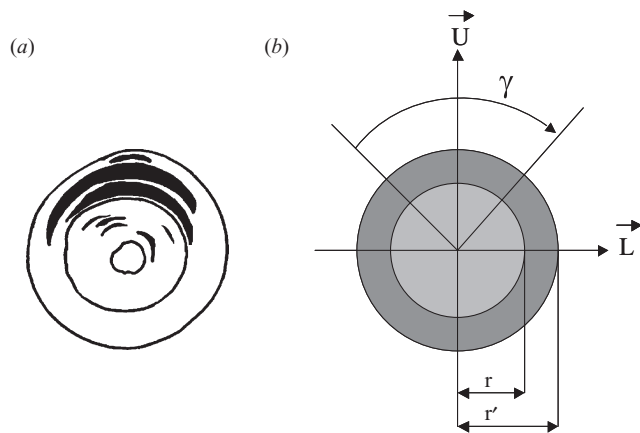


Fig. 6. (a) Presence of reaction wood in the cross-section of a 2-year-old apricot tree shoot, as revealed after Astra-Safranin staining. (b) Schematic representation of a stem cross-section of initial diameter, r , subject to a diameter increase, $\Delta r = r' - r$, with a sector of tension wood in its upper part characterised by its angular extension, γ (from Almérás *et al.* 2004).

the parameter values of the biomechanical model are the same (Fig. 7). Furthermore, MAppleT generates not only the structure and form of trees at a particular developmental stage, but entire developmental sequences. Each sequence can be visualised as a series of images representing different stages of tree development (Fig. 8) or as an animation of development. We observed that trees generated by MAppleT had a visually similar character to a Fuji tree that was digitised and visualised with PlantGL viewer (Pradal *et al.* 2007), at the same development stage (here 6-year-old trees).

To compare simulated and observed trees quantitatively, the architecture of trees generated with L-studio were represented, at the end of each year, as multi-scale tree graph (MTG; Godin and Caraglio 1998), containing both the topological and geometrical information of each plant entity. Several descriptors was extracted, at different scales of observation and then compared between simulated and digitised trees (two digitised Fuji trees were available in the database, see Plant material). For these comparisons, our strategy was to use coarser scales than those at which the model was formulated originally. We then analysed whether the properties that were not specified explicitly in the model would emerge from the system integration.

Regarding tree topology, the main assumption in Markovian models concerned local dependencies between GUs with transition probabilities according to their type and year of growth, and between successive branching zones at the metamer scale. In contrast, no assumption was made regarding the total number of growth units of a given type at the entire tree scale. The corresponding counts thus represent a property of the simulated trees that emerged from the aggregation of the four-state Markov chain and the HSMCs models for branching. These counts cannot be directly calculated from the elementary models and were rather extracted from both simulated and observed trees over 6 successive years. Comparisons of GUs, made separately for terminal and lateral positions, showed that simulation results were most of the time close to field data (Fig. 9). The main pattern related to tree ontogeny, the decrease in the number of long GUs, first in lateral and 1 year later in terminal positions, was correctly simulated. Similarly, the transition from the majority of floral

GUs in lateral positions in the third and fourth years of growth to the majority of floral GUs in terminal positions in the subsequent years was adequately simulated by the model. This change in the floral GU position can be interpreted as a consequence of the decrease in the number of long GUs and the considerable increase in the number of short GUs in the fifth and sixth years.

Regarding geometry, the global shape of the simulated trees emerged from the combination of each particular simulated topology with the biomechanical model. This global shape could not be predicted, as it results from the aggregation of a large number variables and their integration throughout time. To quantify comparisons, several descriptors of shoot geometry, such as the basal diameter, length, inclination or curvature were calculated for both simulated and observed trees. In order to perform a preliminary sensitivity analysis, these descriptors were obtained for different values of seven main parameters of the model (Table 2). Comparisons were made for branches 20 cm in length or more. Both length and basal diameters were underestimated at orders 1 and 2, for all the values of the pipe model exponent and the radius of the leaf petiole. More correct values were obtained at higher orders using the default value $P=2.5$ (data not shown; Fig. 10a). This suggests that other variables such as internode lengths and distal diameters must be further investigated. In particular, the model sensitivity to the variation of apex radius at the beginning of each growing season should be considered. Regarding branch geometry, our analysis mainly focuses on the branch chord inclination (Figs 10b, 11). The independent variation of the seven parameters over 3–7 steps (Table 2) induced a variation of branch chord inclination that ranged from 2 to 30% with respect to that obtained using default values of all parameters (Fig. 11). The parameters that induced the largest variations in branch inclination were the pipe model exponent, petiole radius and Young's modulus. In contrast, the parameters related to fruits (fruit set probability and fruit absolute growth rate) had the lowest impact on branch chord inclination. Moreover, we examined the impact of the pipe model exponent P on branch chord inclination for different branch orders (Fig. 10b). As was the case for the



Fig. 7. Examples of different Fuji apple trees simulated with MAppleT. Differences between these trees reflect the stochastic nature of the topological component of the model.

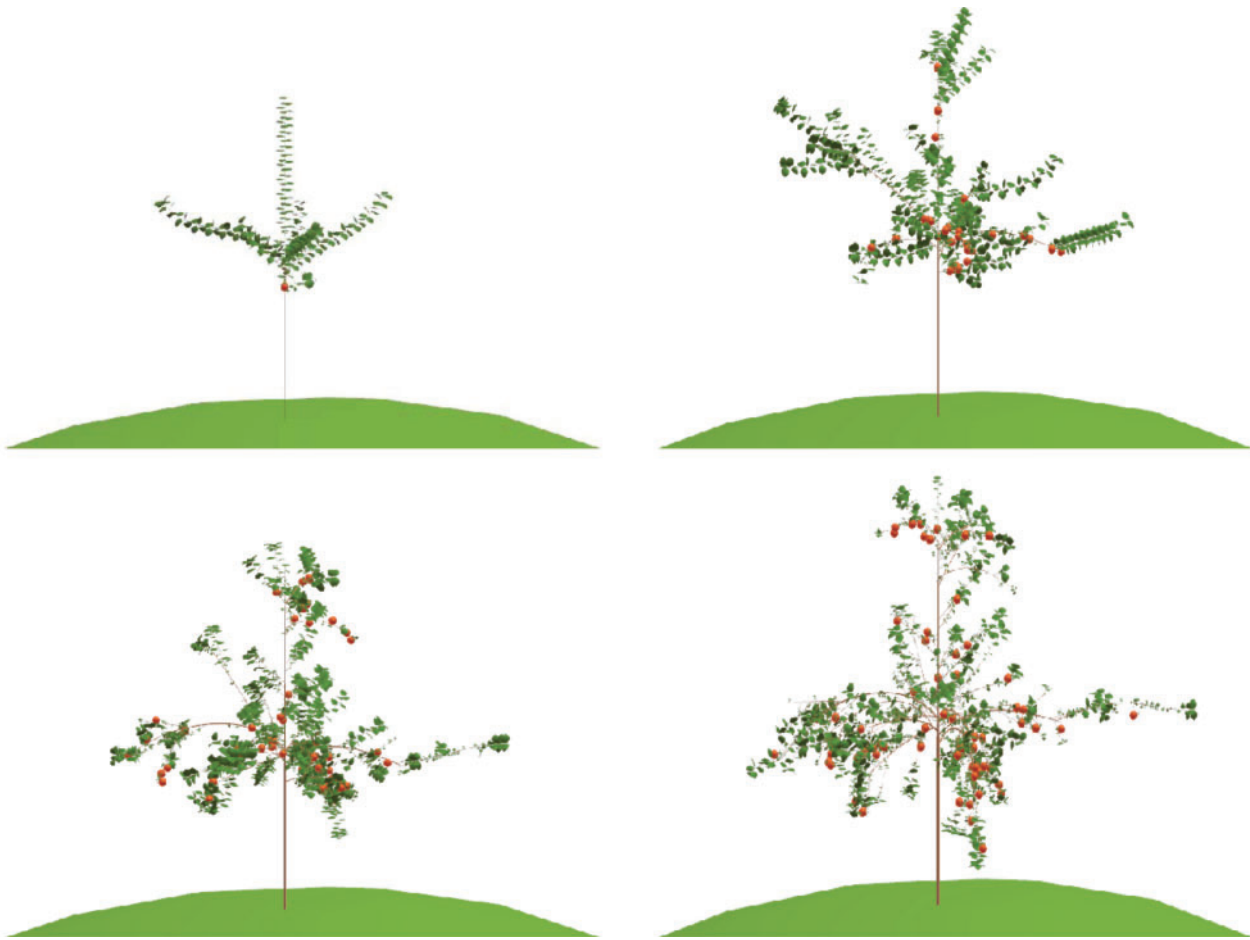


Fig. 8. Year-to-year changes of a typical Fuji apple tree simulated using default values of model parameters. The tree is visualised each year from the second to fifth year of growth, just before harvest time.

branch basal diameter, the mean branch chord inclination was under-estimated for branches of order 1 but it was quite correct for higher orders. At coarser scales, convex hulls that included the fruiting branches and the distal part of the trees were calculated with PlantGL viewer (Fig. 12). The mean value of these hull surfaces compared between simulated and observed trees were in the same range than those obtained when the default value of the pipe model exponent was used in the simulations (data not shown).

Discussion and conclusion

Mixing stochastic and mechanistic model components, MAppleT is a useful tool for simulating the development of apple trees as affected by gravity. A distinctive characteristic of MAppleT is the close connection between the field data and simulations. This connection made it possible to integrate previously existing, but scattered data, and to estimate the model parameters on the basis of observations.

To model tree topology, we used a two-scale stochastic process inspired by previous work (Fine *et al.* 1998). Although only two trees were analysed and the first year of growth were insufficiently characterised, the large number of

GUs and transitions between their types allowed us to estimate the model parameters accurately from the third to the sixth year of growth, as demonstrated by the confidence intervals in Table 1. We note that a related approach has been previously used to simulate plant architectures for computer graphics purposes, but did not take into account the biological background and field data on the modelled plants (Wang *et al.* 2006).

In MAppleT, an efficient strategy was proposed to keep the overall Markovian model parsimonious, based on the study conducted by Renton *et al.* (2006). This strategy relies on the analysis of similarities and discrepancies between branching structures during tree ontogeny. Some parameters (observation distributions) were found to be similar between HSMCs for long and medium GUs, and others (transition probabilities and occupancy distribution) depended on the GU type and year of growth. Since the succession of states is almost deterministic in the case of apple tree (Fig. 1), the underlying ‘left-right’ semi-Markov chain is degenerate: for each state i , (except the ‘end’ state), $q_{ii+1} = 1$ and $q_{ij} = 0$ for $j \neq i + 1$. Hence, there are very few independent transition probabilities. Moreover, the branching zone modelled by state 2 in the HSMC shown in Fig. 1 only occurs in the first 2 years of growth (Renton *et al.* 2006). Thus this

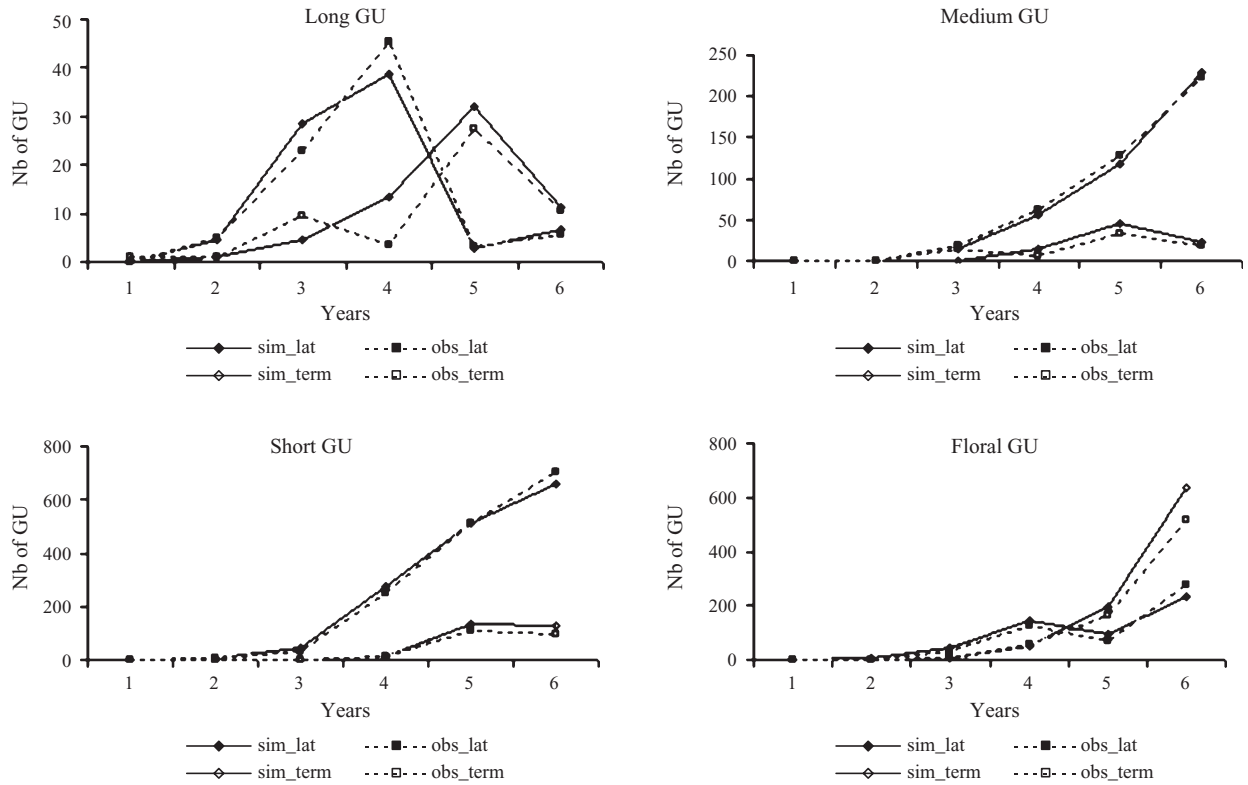


Fig. 9. Confrontation of number of GUs per type between simulated and observed Fuji apple trees. GUs in lateral (lat) and terminal (term) positions were distinguished.

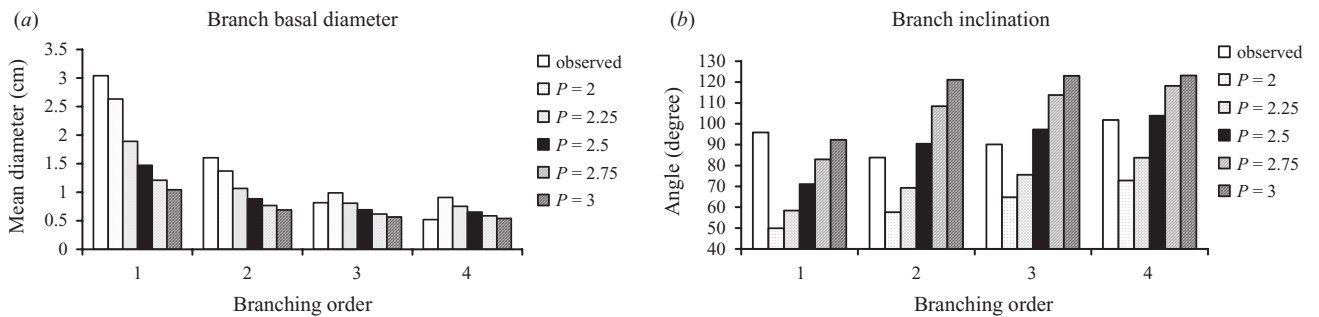


Fig. 10. Examples of geometrical descriptors of apple tree branches (axes that were more than 20 cm) with respect to their branching order. (a) Branch basal diameter and (b) branch inclination were extracted from MTG of apple trees simulated with different values of the pipe model exponent (P) and compared with the equivalent mean values extracted from MTG of two digitised Fuji trees (observed).

state 2 is systematically skipped, except for long GUs in the first 2 years. This leads to another decrease in the number of parameters.

Branching sequences generated by the HSMCs for long and medium GUs are filtered (either accepted or rejected) according to a length criterion. We are aware that this strategy is not optimal and is likely to introduce a bias into the branching sequences. In future work, we intend to improve this estimation strategy in order to obtain a family of HSMCs that realises a better compromise between the fit to the data and the parsimony of the overall family of HSMCs. Sophisticated parameterisations could be proposed,

including (i) tied parameters between HSMCs, (ii) covariates that influence specific parameters (e.g. year of growth influencing transition distributions).

The model simulates the effect of gravity on the plant form, yielding simulated tree forms that are visually similar to the observed trees. However, the effect of gravity on morphogenesis (gravimorphism) is only partly introduced. The median location of long and medium lateral GUs along the parent GU that has been interpreted as a result from bending by Renton *et al.* (2006), is taken into account in MAppleT through the HSMC models for branching. In further developments of the

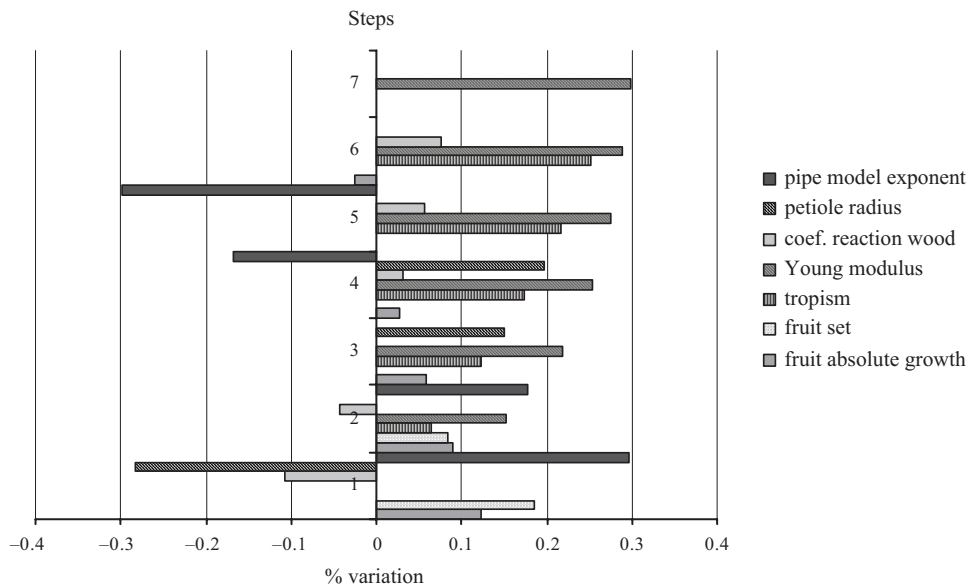


Fig. 11. Percentage of variation induced on branch cord inclination by the independent variation of seven parameters. For each parameter 3–7 steps were explored, the other parameters being fixed to their default value (see Table 2).

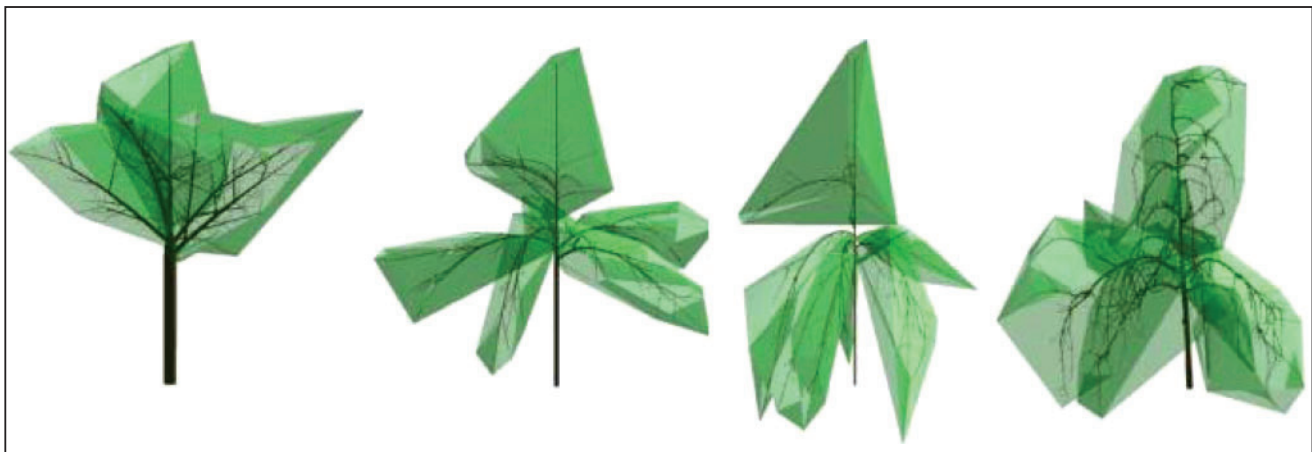


Fig. 12. Envelopes calculated on fruiting branches and top part of the trunk of a tree simulated with three different values of the pipe exponent P ($P=2, 2.5$ and 3 from the left to the right, respectively) and compared with a digitised Fuji tree (last tree on the right).

model, the purely stochastic description of branching should be augmented by a causal feedback between shoot bending and lateral development.

As mentioned above, the present study is closely linked to several field observations. In the case of tree 3-D geometry, available databases allowed us to perform extensive comparisons between simulated and observed trees. These comparisons revealed some discrepancies between the observations and model outputs. For instance, branch inclination for some orders is not simulated correctly (Fig. 8). This may be related to our use of a constant value for the pipe model exponent, independent of the shoot type and

branching order. One approach to improve our results may be based on a refinement of the pipe model, as proposed by Deckmyn *et al.* (2006) or on the introduction of a carbon allocation model such as that used in L-Peach (Lopez *et al.* 2008, this issue).

Although a large number of field observations was used in the present study, more precise estimated or direct measurements might be necessary for some parameters, such as those used for calculating the radial portion of the outermost cambial layer that became reaction wood, which presently come from Alméras' study on apricot tree (Alméras *et al.* 2002). Furthermore, the model is stochastic in nature which makes it necessary to use a

statistical methodology for its validation. It is noticeable that a methodology to perform the model validation on objective bases is currently missing for functional–structural plant model validation. Despite these limitations, MAppleT is one of the first attempt to simulate a fruit tree that develops over years with a global shape reacting to gravity. With L-Peach (Allen *et al.* 2005; Lopez *et al.* 2008, this issue), MAppleT contributes to the foundation of innovative tools for fruit tree simulation. Considering that tree responses to gravity, via the induced changes in tree geometry, have an impact on light interception, within-tree micro-climate, and fruit production and quality, MAppleT will allow further investigations on horticultural practices, as recently initiated by Lopez *et al.* (2008, this issue). Moreover, the genetic variation of shoot morphology that has been demonstrated in the apple tree (Segura *et al.* 2007) could also be simulated through virtual scenario. From a methodological point of view, the proposed modelling approach, which aggregates stochastic and mechanistic models, and the proposed first validation of the model outputs, that includes tree topology and global shape changes in response to gravity, are likely to find applications in other plants as well.

Acknowledgements

We thank Julia Taylor-Hell for kindly making her model of branch bending in poplar trees available. We also thank Frédéric Boudon for his assistance on the Geom module from PlantGL, Jean-Jacques Kelner and Jean-Luc Regnard for allowing us to use their observations of apple trees. This research was supported in part by the Natural Sciences and Engineering Research Council of Canada Discovery Grant RGPIN 130084–2008 to PP. The postdoctoral positions of C Smith and M Renton were granted by the INRA Department of Genetics and Plant Breeding.

References

- Adam B, Sinoquet H, Godin C (1999) '3A version 1.0: Un logiciel pour l'Acquisition de l'Architecture des Arbres, intégrant la saisie simultanée de la topologie au format AMAPmod et de la géométrie par digitalisation 3D. Guide de l'utilisateur.' (INRA-PIAF Clermont-Ferrand: France)
- Allen M, Prusinkiewicz P, Dejong T (2005) Using L-systems for modeling source–sink interactions, architecture and physiology of growing trees: the L-PEACH model. *New Phytologist* **166**, 869–880. doi: 10.1111/j.1469-8137.2005.01348.x
- Alméras T (2001) Acquisition de la forme des axes ligneux d'un an chez trois variétés d'abricotier: confrontation de données expérimentales à un modèle biomécanique, PhD Thesis, SupAgro Montpellier University, Montpellier.
- Alméras T, Gril J, Costes E (2002) Bending of apricot-tree branches under the weight of axillary productions: confrontation of a mechanical model to experimental data. *Trees* **16**, 5–15.
- Alméras T, Costes E, Salles JC (2004) Identification of biomechanical factors involved in stem form variability between apricot tree varieties. *Annals of Botany* **93**, 455–468. doi: 10.1093/aob/mch054
- Ancelet P, Fourcaud T, Lac P (2004) Modelling the biomechanical behaviour of growing trees at the forest stand scale. Part I: Development of an incremental transfer matrix method and application to simplified tree structures. *Annals of Forest Science* **61**, 263–275. doi: 10.1051/forest:2004019
- Benzing S (1999) Patterns of vegetative and reproductive growth in apple (*Malus × domestica* Borkh.). Master thesis, Faculty de Wiesbaden, Geisenheim.
- Costes E, Guédon Y (2002) Modelling branching patterns on 1-year-old trunks of six apple cultivars. *Annals of Botany* **89**, 513–524. doi: 10.1093/aob/mcf078
- Costes E, Lauri PÉ (1995) Processus de croissance en relation avec la ramification sylleptique et la floraison chez le pommier. In 'Architecture des arbres fruitiers et forestiers'. (Ed. J Bouchon) pp. 41–50. (INRA Editions: Paris)
- Costes E, Lauri PE, Lespinasse JM (1995) Modélisation de la croissance et de la ramification chez quelques cultivars de Pommier. In 'Architecture des arbres fruitiers et forestiers'. (Ed. J Bouchon) pp. 27–39. (INRA Editions: Paris)
- Costes E, Fournier D, Salles JC (2000) Changes in primary and secondary growth as influenced by crop load effects in 'Fantasme' apricot trees. *Journal of Horticultural Science & Biotechnology* **75**, 510–529.
- Costes E, Sinoquet H, Kelner JJ, Godin C (2003) Exploring within-tree architectural development of two apple tree cultivars over 6 years. *Annals of Botany* **91**, 91–104. doi: 10.1093/aob/mcg010
- Costes E, Lauri PE, Régnard JL (2006) Tree architecture and production. *Horticultural Reviews* **32**, 1–60.
- Crabbé J, Escobedo-Alvarez JA (1991) Activités méristématiques et cadre temporel assurant la transformation florale des bourgeons chez le Pommier (*Malus × domestica* Borkh., cv. golden delicious). *L'Arbre: Biologie et Développement: Naturalia Monspeliensia Special no*, 369–379.
- Deckmyn G, Evans SP, Randle TJ (2006) Refined pipe theory for mechanistic modeling of wood development. *Tree Physiology* **26**, 703–717.
- Durand J-B, Guédon Y, Caraglio Y, Costes E (2005) Analysis of the plant architecture via tree-structured statistical models: the hidden Markov tree models. *New Phytologist* **166**, 813–825. doi: 10.1111/j.1469-8137.2005.01405.x
- Fine S, Singer Y, Tishby N (1998) The hierarchical hidden Markov model: analysis and applications. *Machine Learning* **32**, 41–62. doi: 10.1023/A:1007469218079
- Fournier M (1989) Mécanique de l'arbre sur pied: maturation, poids propre, contraintes climatiques dans la tige standard. PhD thesis, INP de Lorraine, Nancy.
- Fournier M, Chanson B, Guitard D, Thibaut B (1991a) Mechanics of standing trees: modelling a growing structure submitted to continuous and fluctuating loads. 1. Analysis of support stresses. *Annals of Forest Science* **48**, 513–525. doi: 10.1051/forest:19910503
- Fournier M, Chanson B, Guitard D, Thibaut B (1991b) Mechanics of standing trees: modelling a growing structure submitted to continuous and fluctuating loads. 2. Tridimensional analysis of maturation stresses. *Annals of Forest Science* **48**, 527–546. doi: 10.1051/forest:19910504
- Gautier H, Mech R, Prusinkiewicz P, Varlet-Grancher C (2000) 3-D architectural modelling of aerial photomorphogenesis in white clover (*Trifolium repens* L.) using L-systems. *Annals of Botany* **85**, 359–370. doi: 10.1006/anbo.1999.1069
- Godin C (2000) Representing and encoding plant architecture: a review. *Annals of Forest Science* **57**, 413–438. doi: 10.1051/forest:2000132
- Godin C, Caraglio Y (1998) A multiscale model of plant topological structures. *Journal of Theoretical Biology* **191**, 1–46. doi: 10.1006/jtbi.1997.0561
- Godin C, Costes E, Sinoquet H (1999) A method for describing plant architecture which integrates topology and geometry. *Annals of Botany* **84**, 343–357. doi: 10.1006/anbo.1999.0923
- Goldstein H (1980) 'Classical mechanics.' 2nd edn. (Addison-Wesley: Reading, UK)
- Guédon Y (2003) Estimating hidden semi-Markov chains from discrete sequences. *Journal of Computational and Graphical Statistics* **12**, 604–639. doi: 10.1198/1061860032030

- Guédon Y, Barthélémy D, Caraglio Y, Costes E (2001) Pattern analysis in branching and axillary flowering sequences. *Journal of Theoretical Biology* **212**, 481–520. doi: 10.1006/jtbi.2001.2392
- Hallé F, Martin R (1968) Etude de la croissance rythmique chez l'hévéa (*Hévéa brasiliensis* Müll-Arg. *Euphorbiacées-Crotonoïdées*). *Adansonia Ser.* **2**, 475–503.
- Hanan J, Hearn AB (2002) Linking physiological and architectural models of cotton. *Agricultural Systems* **14**, 1–31.
- Hanan J, Room P (1997) Practical aspects of virtual plant research. In 'Plants to ecosystems'. (Ed. MT Michalewicz) pp. 28–45. (CSIRO Publishing: Melbourne)
- Hangarter RP (1997) Gravity, light and plant form. *Plant, Cell & Environment* **20**, 796–800. doi: 10.1046/j.1365-3040.1997.d01-124.x
- Jirasek C, Prusinkiewicz P, Moulia B (2000) Integrating biomechanics into developmental plant models expressed using L-systems. In 'Plant biomechanics 2000'. (Eds HC Spatz, T Speck) pp. 615–624. (Georg Thieme Verlag: Freiburg-Badenweiler)
- Lakso AN, Grappadelli LC, Barnard J, Goffinet MC (1995) An exponential model of the growth pattern of the apple fruit. *Journal of Horticultural Science* **70**, 389–394.
- Landau LD, Lifshitz EM (1986) 'Theory of elasticity.' 3rd Edn. (Butterworth-Heinemann: Oxford, UK)
- Lauri PÉ (2002) From tree architecture to tree training – an overview of recent concepts developed in apple in France. *Journal of the Korean Society for Horticultural Science* **43**, 782–788.
- Lauri PÉ, Térout E, Lespinasse JM (1997) Relationship between the early development of apple fruiting branches and the regularity of bearing – an approach to the strategies of various cultivars. *Journal of Horticultural Science* **72**, 519–530.
- Lindenmayer A (1968) Mathematical models for cellular interaction in development, Part I and II. *Journal of Theoretical Biology* **18**, 280–315. doi: 10.1016/0022-5193(68)90079-9
- Lopez G, Favreau RR, Smith C, Costes E, Prusinkiewicz P, DeJong PM (2008) Integrating simulation of architectural development and source-sink behaviour of peach trees by incorporating Markov chains and physiological organ function sub-models into L-PEACH. *Functional Plant Biology* **35**, 761–771.
- MacDonald N (1983) 'Trees and networks in biological models.' (J. Wiley & Sons: Chichester, UK)
- Massonnet C (2004) Variabilité architecturale et fonctionnelle du système aérien chez le pommier (*Malus × Domestica* Borkh.): comparaison de quatre cultivars par une approche de modélisation structure-fonction. PhD Thesis, SupAgro Montpellier University, Montpellier.
- Matsuzaki J, Masumori M, Takeshi T (2007) Phototropic bending of non-elongating and radially growing stems results from asymmetrical xylem formation. *Plant, Cell & Environment* **30**, 646–653. doi: 10.1111/j.1365-3040.2007.01656.x
- Mech R, Prusinkiewicz P (1996) Visual models of plants interacting with their environment. In 'Proceedings of SIGGRAPH 96, New Orleans, Louisiana, 4–9 August 1996'. pp. 397–410. (ACM SIGGRAPH: New York)
- Murray C (1927) A relationship between circumference and weight in trees and its bearing on branching angles. *Journal of General Physiology* **10**, 725–729. doi: 10.1085/jgp.10.5.725
- Niklas K (1992) 'Plant biomechanics. An engineering approach to plant form and function.' (The University of Chicago Press: Chicago)
- Pradal C, Boudon F, Nouguier C, Chopard J, Godin C (2007). PlantGL: a Python-based geometric library for 3D plant modelling at different scales. INRIA Research Report no. 6367. Available at <http://www-sop.inria.fr/virtualplants/Publications/2007/PBNCG07/>. [Verified 2 September 2008]
- Prusinkiewicz P (1998) Modeling of spatial structure and development of plants. *Scientia Horticulturae* **74**, 113–149. doi: 10.1016/S0304-4238(98)00084-3
- Prusinkiewicz P, Lindenmayer A (1990) 'The algorithmic beauty of plants.' (Springer-Verlag: New York)
- Prusinkiewicz P, Mündermann L, Karwowski R, Lane B (2001) The use of positional information in the modeling of plants. *Proceedings of the 28th Annual Conference on Computer Graphics And Interactive Techniques* **20**, 289–300. doi: 10.1145/383259.383291
- Prusinkiewicz P, Karwowski R, Lane B (2007) The L + C plant-modelling language. In 'Functional-structural plant modeling in crop production'. (Eds J Vos, LFM de Visser, PC Struick, JB Evers) pp. 27–42. (Springer-Verlag: Wageningen, The Netherlands)
- Renton M, Kaitaniemi P, Hanan J (2005a) Functional-structural plant modelling using a combination of architectural analysis, L-systems and a canonical model of function. *Ecological Modelling* **184**, 277–298. doi: 10.1016/j.ecolmodel.2004.10.008
- Renton M, Hanan J, Burrage K (2005b) Using the canonical modelling approach to simplify the simulation of function in functional-structural plant models. *New Phytologist* **166**, 845–857. doi: 10.1111/j.1469-8137.2005.01330.x
- Renton M, Guédon Y, Godin C, Costes E (2006) Similarities and gradients in growth unit branching patterns during tree ontogeny based on a stochastic approach in 'Fuji' apple trees. *Journal of Experimental Botany* **57**, 3131–3143. doi: 10.1093/jxb/erl075
- Segura V, Denancé C, Durel CE, Costes E (2007) Wide range QTL analysis for complex architectural traits in a 1-year-old apple progeny. *Genome* **50**, 159–171. doi: 10.1139/G07-002
- Shinozaki K, Yoda K, Hozumi K, Tira T (1964) A quantitative analysis of plant form – the pipe model theory. (i) Basic analyses. *Japanese Journal of Ecology* **14**, 97–105.
- Sinoquet H, Rivet P, Godin C (1997) Assessment of the three-dimensional architecture of walnut trees using digitising. *Silva Fennica* **31**, 265–273.
- Suzuki M, Hiura T (2000) Allometric differences between current-year shoots and large branches of deciduous broad-leaved tree species. *Tree Physiology* **20**, 203–209.
- Taylor-Hell J (2005) Biomechanics in botanical trees. Master thesis, University of Calgary, Calgary.
- Thornby D, Renton M, Hanan J (2003) Using computational plant science tools to investigate morphological aspects of compensatory growth. *Computational Science – ICCS 2003* **2660/2003**, 708–717. doi: 10.1007/3-540-44864-0_73
- Wang R, Hua W, Dong Z, Peng Q, Bao H (2006) Synthesizing trees by plantons. *The Visual Computer* **22**, 238–248. doi: 10.1007/s00371-006-0002-x
- White J (1979) The plant as a metapopulation. *Annual Review of Ecology and Systematics* **10**, 109–145. doi: 10.1146/annurev.es.10.110179.000545
- Wilson BF, Archer RR (1977) Reaction wood: induction and mechanical action. *Annual Review of Plant Physiology* **28**, 23–43. doi: 10.1146/annurev.pp.28.060177.000323

Manuscript received 17 March 2008, accepted 4 August 2008